

Momentum distribution functions of strongly correlated systems of particles: Wigner approach and path integrals

A S Larkin, V S Filinov and V E Fortov

Joint Institute for High Temperatures of the Russian Academy of Sciences, Izhorskaya 13
Bldg 2, Moscow 125412, Russia

E-mail: vladimir_filinov@mail.ru

Abstract. The new numerical version of the Wigner approach to quantum mechanics for treatment thermodynamic properties of the strongly interacting systems of particles has been developed for extreme conditions, when there are no small physical parameters and analytical approximations used in different kind of perturbation theories can not be applied. The new path integral representation of the quantum Wigner function in the phase space has been developed for canonical ensemble. Explicit analytical expression of the Wigner function has been obtained in linear and harmonic approximations. The new quantum Monte-Carlo method for calculations of average values of arbitrary quantum operators has been proposed. Preliminary calculations of the momentum distribution function of the Coulomb systems of particles have been carried out. Comparison with classical Maxwell–Boltzmann distribution shows the significant influence of quantum effects on the high energy asymptotics (“tails”) of the calculated momentum distribution functions, which resulted in appearance of sharp oscillations.

1. Introduction

Quantum effects can affect the shape of the particle kinetic energy distribution function, as the interaction of a particle with its surroundings restricts the volume of configuration space, which, due to the uncertainty relation, results in an increase in the volume of the momentum space, i.e., in a rise in the fraction of particles with higher momenta. Allowing for quantum effects is important in kinetic consideration of such phenomena as the transition of combustion into detonation, flame propagation, vibrational relaxation, and even thermonuclear fusion at high pressure and low temperatures. Quantum effects are also important in treatment of transport properties of the strongly interacting systems of many particles [1–4].

The direct way to consider the influence of the quantum effects on the kinetic distribution functions is to use the Wigner formulation of quantum mechanics in phase space [5, 6]. The quantum Wigner function is similar to distribution function in classical statistics in phase space. Thereby average values of arbitrary physical quantities can be calculated by formulas, similar to classical statistics. Methods for treatment of the single-particle quantum dynamics in Wigner approach in microcanonical ensemble were proposed in [7–11]. Recently a generalization of these methods to the many-body Wigner equation for distinguishable particles has been done in [12]. This approach is based on Monte Carlo approach for solving the discretized version of



the integral Wigner–Liouville equation. Authors validate this approach by studying the time-dependent evolution of a system containing only two charged particles (wave-packets) in an external potential. Interesting results have been obtained also for the system of two entangled wave-packets. However comparison with independent results has not been done.

In this work we are going to develop the new numerical version of the Wigner approach to quantum mechanics in the phase space for treatment of thermodynamic properties of the strongly interacting many particle systems under extreme conditions, when there are no small physical parameters and analytical approximations used in different kind of perturbation theories can not be applied [13–15]. The new path integral representation of the quantum Wigner function in the phase space has been developed for canonical ensemble. Explicit analytical expression of the Wigner function has been obtained in linear and harmonic approximations. We have developed new quantum Monte-Carlo method for calculations of average values of arbitrary quantum operators. Preliminary calculations of the momentum distribution function for Coulomb system of particles has been carried out. Comparison with classical Maxwell–Boltzmann distribution shows the significant influence of the quantum effects on the high energy asymptotics (“tails”) of the calculated distribution functions resulted in appearance of sharp oscillations.

2. Wigner function for canonical ensemble

The Wigner function $W(p, x; t)$ being the analogue of the classical distribution function in the phase space has a wide range of applications in quantum mechanics. The Wigner function of the many particle system in canonical ensemble is defined as a Fourier transform of the off-diagonal matrix element of density matrix in coordinate representation:

$$W(p, x; \beta) = Z(\beta)^{-1} \int d\xi e^{i(p|\xi\rangle/\hbar} \langle x - \xi/2 | e^{-\beta \hat{H}} | x + \xi/2 \rangle. \quad (1)$$

Here we are going to obtain new representation of Wigner functions in the path integral form [16–18], which allows the numerical simulations of strongly coupled quantum systems of particles in canonical ensemble. Since operators of kinetic and potential energy in Hamiltonian do not commute, the exact explicit analytical expression for Wigner function does not exist in general. To overcome this difficulty let us represent Wigner function similarly to path integral representation of the partition function [5, 16, 18]. As example of Coulomb system of particles, we consider a 3D two-component strongly asymmetric electron–hole plasma consisting of $N_e = N_h = N$ electrons and heavy holes in equilibrium [19]. The hamiltonian of the system $\hat{H} = \hat{K} + \hat{U}^c$ contains kinetic energy \hat{K} and Coulomb interaction energy $\hat{U}^c = \hat{U}_{hh}^c + \hat{U}_{ee}^c + \hat{U}_{eh}^c$ contributions. The thermodynamic properties in the canonical ensemble with given temperature T and fixed volume V are fully described by the diagonal elements of the density operator $\hat{\rho} = e^{-\beta \hat{H}}/Z$ with the partition function (normalization constant)

$$Z(N_e, N_h, V; \beta) = \frac{1}{N_e! N_h!} \sum_{\sigma} \int_V dx \rho(x, \sigma; \beta), \quad (2)$$

where $\beta = 1/k_B T$, and $\rho(x, \sigma; \beta)$ denotes the diagonal matrix elements of the density operator. In equation (2), $x = \{x_e, x_h\}$ and $\sigma = \{\sigma_e, \sigma_h\}$ are the spatial coordinates and spin degrees of freedom of the electrons and holes, i.e. $x_a = \{x_{1,a} \dots x_{l,a} \dots x_{N_a,a}\}$ and $\sigma_a = \{\sigma_{1,a} \dots \sigma_{l,a} \dots \sigma_{N_a,a}\}$, with $a = e, h$.

In order to calculate thermodynamic functions, the logarithm of the partition function has to be differentiated with respect to thermodynamic variables. For example, for pressure and

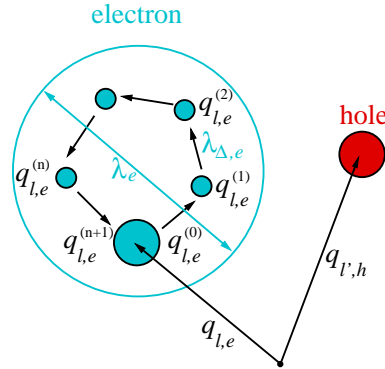


Figure 1. Beads representation of electrons and holes. Here $\lambda_e^2 = 2\pi\hbar^2\beta/m_e$, $\lambda_{\Delta,e}^2 = 2\pi\hbar^2\Delta\beta/m_e$, $x_{l,e}^{(1)} = x_{l,e}^{(0)} + \lambda_{\Delta,e}\eta_{l,e}^{(1)}$, and $\sigma = \sigma'$. The holes have a similar beads representation, however $\lambda_{\Delta,h}^2$ is (m_h/m_e) -times smaller, so their beads distribution is not resolved in the figure.

internal energy follows

$$\beta p = \frac{\partial \ln Z}{\partial V} = \left[\frac{\alpha}{3V} \frac{\partial \ln Z}{\partial \alpha} \right]_{\alpha=1}, \quad (3)$$

$$\beta E = -\beta \frac{\partial \ln Z}{\partial \beta}, \quad (4)$$

where $\alpha = L/L_0$ is a length scaling parameter.

Of course, the exact density matrix of interacting quantum systems is not known (particularly for low temperatures and high densities), but it can be constructed using a path integral approach [16,18] based on the operator identity $e^{-\beta\hat{H}} = e^{-\epsilon\hat{H}} \cdot e^{-\epsilon\hat{H}} \dots e^{-\epsilon\hat{H}}$, where $\epsilon = \beta/M$, which allows us to rewrite the integral in equation (2)

$$\sum_{\sigma} \int dx^{(0)} \rho(x^{(0)}, \sigma; \beta) = \int dx^{(0)} \dots dx^{(m)} \dots dx^{(M-1)} \rho^{(1)} \cdot \rho^{(2)} \dots \rho^{(M-1)} \times \quad (5)$$

$$\sum_{\sigma} \sum_{P_e} \sum_{P_h} (\pm 1)^{\kappa_{P_e} + \kappa_{P_h}} \mathcal{S}(\sigma, \hat{P}_e \hat{P}_h \sigma') \hat{P}_e \hat{P}_h \rho^M \big|_{q^M = q^{(0)}, \sigma' = \sigma}.$$

The spin gives rise to the spin part of the density matrix (\mathcal{S}) with exchange effects accounted for by the permutation operators \hat{P}_e and \hat{P}_h acting on the electron and hole coordinates x^M and spin projections σ' . The sum is over all permutations with parity κ_{P_e} and κ_{P_h} . In equation (6) the index $m = 0, \dots, M-1$ labels the off-diagonal high-temperature density matrices $\rho^{(m+1)} \equiv \rho(x^{(m)}, x^{(m+1)}; \epsilon) = \langle x^{(m)} | e^{-\epsilon\hat{H}} | x^{(m+1)} \rangle$. In this paper we are going to consider strongly coupled non-degenerate plasma, so the main contribution in the sum over permutations comes from the identical permutations and each particle is represented by a closed trajectory consisting of a set of M coordinates (“beads”). So the whole configuration of the particles is represented by a $3(N_e + N_h)M$ -dimensional vector $\tilde{x} \equiv \{x_{1,e}^{(0)}, \dots, x_{1,e}^{(M-1)}, x_{2,e}^{(0)}, \dots, x_{2,e}^{(M-1)}, \dots, x_{N_e,e}^{(M-1)}; x_{1,h}^{(0)}, \dots, x_{N_h,h}^{(M-1)}\}$. Figure 1 illustrates the representation of one (light) electron and one (heavy) hole. The circle around the electron beads symbolizes the region that mainly contributes to the partition function path integral. The size of this region is of the order of the thermal electron wavelength $\lambda_e(T)$, while typical distances between electron beads are of the order of the electron wavelength taken at an M -times higher

temperature. The same representation is valid for each hole but it is not shown since, due to the larger hole mass, the characteristic length scales are substantially smaller. However, in the simulations discussed below the holes are treated according to the full beads representation.

2.1. High-temperature asymptotics for the density matrix. Kelbg potential

In this section we discuss approximations for the high-temperature density matrix which can be used for efficient direct path integral Monte Carlo (PIMC) simulations. It involves effective quantum pair potentials Φ_{ab} , which are approximated by the Kelbg potential. Here, we closely follow earlier work [20] where details and further references can be found.

2.1.1. Pair approximation and Kelbg potential The N-particle high-temperature density matrix is expressed in terms of two-particle density matrices (higher order terms become negligible at sufficiently high temperature, i.e. for large number M of time slices) given by

$$\begin{aligned} \rho_{ab}(x_{p,a}, x'_{p,a}, x_{t,b}, x'_{t,b}; \beta) &= \frac{(m_a m_b)^{3/2}}{(2\pi\hbar\beta)^3} \exp\left[-\frac{m_a}{2\hbar^2\beta}(x_{p,a} - x'_{p,a})^2\right] \times \\ &\times \exp\left[-\frac{m_b}{2\hbar^2\beta}(x_{t,b} - x'_{t,b})^2\right] \exp[-\beta\Phi_{ab}^{\text{OD}}]. \end{aligned} \quad (6)$$

This results from factorization into kinetic and interaction parts, $\rho_{ab} \approx \rho_0^K \rho_{ab}^U$, which is exact in the classical case, i.e. at sufficiently high temperature. The error made at finite temperature vanishes with the number of time slices as M^{-2} [20]. The off-diagonal density matrix element (6) involves an effective pair interaction which is expressed approximately via its diagonal elements, $\Phi_{ab}^{\text{OD}}(x_{p,a}, x'_{p,a}, x_{t,b}, x'_{t,b}; \beta) \approx [\Phi_{ab}(x_{p,a} - x_{t,b}; \beta) + \Phi_{ab}(x'_{p,a} - x'_{t,b}; \beta)]/2$, for which we use the familiar Kelbg potential [21, 22]

$$\Phi_{ab}(x_{ab}; \epsilon) = \frac{e_a e_b}{\lambda_{ab} x_{ab}} \left[1 - e^{-x_{ab}^2} + \sqrt{\pi} x_{ab} (1 - \text{erf}(x_{ab})) \right], \quad (7)$$

where $x_{ab} = |x_{p,a} - x_{t,b}|/\lambda_{ab}$, $\lambda_{ab} = \sqrt{\hbar^2\epsilon/(2m_{ab})}$, $m_{ab} = m_a m_b/(m_a + m_b)$ is the reduced mass of the (ab) -pair of particles and the error function is defined by $\text{erf}(x) = \frac{2}{\sqrt{\pi}} \int_0^x dt e^{-t^2}$.

Note that the Kelbg potential is finite at zero distance which is a consequence of quantum effects. The validity of this potential as well as its the off-diagonal approximation is restricted to temperatures substantially higher than the exciton binding energy [23, 24] which puts another lower bound on the number of time slices n . For a discussion of other effective potentials, we refer to [20, 23–25].

Summarizing the above approximations, we can conclude that with the approximations (6,7) each of the high-temperature factors on the r.h.s. of equation (6), carries an error of the order $1/M^2$. Within these approximations, we obtain the result

$$\rho^{(m)} = \rho_0^{(m)} e^{-\epsilon U(x^{(m-1)})} \delta(x^{(m-1)} - x^{(m)}) + \mathcal{O}[(1/M)^2], \quad (8)$$

where $\rho_0^{(m)}$ is the kinetic density matrix, and U denotes the sum of all interaction energies, each consisting of the respective sum of pair interactions given by Kelbg potentials, $U(x^{(m)}) = U_{hh}(x_h^{(m)}) + U_{ee}(x_e^{(m)}) + U_{eh}(x_h^{(m)}, x_e^{(m)})$.

2.2. Path integral representation of Wigner function

As in the previous section we represent statistical operator $e^{-\beta\hat{H}}$ as product of large number M operators $e^{-\epsilon\hat{H}}$ formally related to high temperature ($\epsilon = \beta/M$), so we can write Wigner

function in form of multiple integral of the product of the high temperature density matrices (see equation (1)):

$$W(p, x; \beta) = Z(\beta)^{-1} \int d\xi e^{i\langle p|\xi\rangle/\hbar} \int dx^{(1)} \dots dx^{(M-1)} \times \left[\prod_{m=0}^{M-1} \langle x^{(m)} | e^{-\epsilon \hat{H}} | x^{(m+1)} \rangle \right] \Big|_{x^{(0)}=x-\xi/2, x^{(M)}=x+\xi/2}. \quad (9)$$

For simplicity we have omitted spin variable. As before making use of the Kelbg potential the explicit expression of the high temperature density matrices can be calculated with accuracy up to $O(\epsilon^2)$ in the limit $\epsilon \rightarrow 0$ [18]:

$$\langle x | e^{-\epsilon \hat{H}} | y \rangle \approx \lambda_\epsilon^{-1} \exp \left[-\pi \lambda_\epsilon^{-2} \langle x - y | x - y \rangle - \epsilon U(x) \right]. \quad (10)$$

Here angle brackets means scalar product of two vectors, while here and further the symbol $\lambda_\epsilon^{-2} \langle a|b \rangle$ means that each term in scalar product $\langle a|b \rangle$ is normalized by the electron or hole thermal wavelength respectively and $\lambda_\epsilon = \sqrt{\frac{2\pi\hbar^2\epsilon}{m}}$ is taken at high temperature $M \cdot T$. Now replacing variables of integration:

$$x^{(m)} = x_m - \frac{\xi}{2} \frac{M-2m}{M}, \quad (11)$$

we obtain

$$W(p, x; \beta) = Z(\beta)^{-1} C(M) \frac{1}{\lambda^M} \int d\xi \int dx_1 \dots dx_{M-1} \exp \left\{ \frac{i}{\hbar} \langle p|\xi \rangle - \frac{\pi \langle \xi|\xi \rangle}{\lambda^2} - \sum_{m=0}^{M-1} \left[M \frac{\pi}{\lambda^2} \langle x_{m+1} - x_m | x_{m+1} - x_m \rangle + \epsilon U \left(x_m - \frac{\xi}{2} \left(1 - 2 \frac{m}{M} \right) \right) \right] \right\} \Big|_{x_0=x_M=x}.$$

Here $C(M) = M^{-M/2}$ depends only on number M . As it will be shown further, this constant is canceled in calculations of average values of operators.

It is convenient to use dimensionless variables $\bar{\xi}$ and $\bar{x}_1, \dots, \bar{x}_{M-1}$: $\xi = \lambda \bar{\xi}$, $x_m = \lambda \bar{x}_m$. Using designation $\bar{\epsilon} = 1/M$, we obtain the next expression for Wigner function:

$$W(p, x; \beta) = C(M) Z(\beta)^{-1} \int d\bar{\xi} \int d\bar{x}_1 \dots d\bar{x}_{M-1} \exp \left\{ \frac{i}{\hbar} \langle p\lambda|\bar{\xi} \rangle - \pi \langle \bar{\xi}|\bar{\xi} \rangle - \sum_{m=0}^{M-1} \left[\pi \frac{\langle \bar{x}_{m+1} - \bar{x}_m | \bar{x}_{m+1} - \bar{x}_m \rangle}{\bar{\epsilon}^2} + \beta U \left(\lambda \bar{x}_m - \lambda \frac{\bar{\xi}}{2} (1/2 - \bar{\epsilon} m) \right) \right] \right\} \Big|_{\bar{x}_0=\bar{x}_M=x/\lambda}. \quad (12)$$

When $\bar{\epsilon} \rightarrow 0$ this multiple integral turns to exact representation of the Wigner function $W(p, x; \beta)$ in the form of path integral with continuous dimensionless 'time' τ , which corresponds to $\bar{\epsilon} m$ in discrete case. Also set of independent variables \bar{x}_m turns into closed trajectory $\bar{x}(\tau)$. This trajectory starts and ends in point x/λ when $\tau = 0$ and 1. In this limit expression $\frac{\bar{x}_{m+1} - \bar{x}_m}{\bar{\epsilon}}$ is nothing else than derivative $\frac{d\bar{x}}{d\tau}$, which we denote as $\dot{\bar{x}}(\tau)$.

As a result, we have a new exact representation of Wigner function for canonical ensemble in form of path integral:

$$W(p, x; \beta) = Z(\beta)^{-1} \int d\bar{\xi} \exp \left\{ i \frac{\langle p\lambda | \bar{\xi} \rangle}{\hbar} - \pi \langle \bar{\xi} | \bar{\xi} \rangle \right\} \times \quad (13)$$

$$\times \int_{\bar{x}(0)=\bar{x}(\tau)=x/\lambda} D\bar{x}(\tau) \exp \left\{ - \int_0^1 d\tau \left[\pi \langle \dot{\bar{x}}(\tau) | \dot{\bar{x}}(\tau) \rangle + \beta U(\lambda \bar{x}(\tau) + \lambda \bar{\xi}(\tau - 1/2)) \right] \right\}.$$

where symbol $|\lambda a\rangle$ means that in vector $|a\rangle$ each component is multiplied on related electron or hole thermal wave length $\lambda = \sqrt{\frac{2\pi\hbar^2\beta}{m}}$. Let us note that integration here relates to the integration over the Wiener measure of all closed trajectories $\bar{x}(\tau)$. Variable $\bar{\xi}$ is integrand in Fourier transform. In fact, a particle is presented by the closed trajectory with characteristic size of order λ in coordinate space. This is manifestation of the uncertainty principle.

2.3. Harmonic approximation for Wigner function

The expression for Wigner function (13) is inconvenient practically because the momentum p is connected with other variables only through Fourier transform. Even in case of free particle ($V(x) = 0$) this expression does not explicitly contain the analytic expression of Maxwell–Boltzmann distribution. To obtain it explicitly, we have to integrate over variable $\bar{\xi}$. In general case this integral can not be calculated analytically. Exclusions are the linear or harmonic potentials, when power of variable $\bar{\xi}$ is not more than two.

To do this integration analytically and to obtain explicit expression for Wigner function let us take the approximation for potential $V(x)$ arising from the Taylor expansion up to the first or second order in the $\bar{\xi}$:

$$U(\lambda \bar{x}(\tau) + \lambda \bar{\xi}(\tau - 1/2)) \approx U(\lambda \bar{x}(\tau)) + \langle \lambda \bar{\xi}(\tau - 1/2) | \frac{\partial U(x)}{\partial x} \rangle \Big|_{x=\lambda \bar{x}} +$$

$$+ \frac{1}{2} \langle \lambda \bar{\xi}(\tau - 1/2) | \frac{\partial^2 U(x)}{\partial x^2} | \lambda \bar{\xi}(\tau - 1/2) \rangle \Big|_{x=\lambda \bar{x}(\tau)}. \quad (14)$$

Here the second term means scalar product of the vector proportional to $\bar{\xi}$ and the multidimensional gradient of pseudopotential energy, while third term means quadratic form with the matrix of the second derivatives.

If we take into account all terms in expansion (14), the expression for Wigner function (13) takes the form of gaussian integral over variable $\bar{\xi}$ and the final expression for Wigner function in harmonic approximation can be written in the following form:

$$W(p, x; \beta) = Z(\beta)^{-1} \int_{z(0)=z(\tau)=0} Dz(\tau) \chi[x, z]^{-\frac{1}{2}} \times$$

$$\times \exp \left\{ - \frac{\beta}{2m} \langle p | \chi^{-1}[x, z] | p \rangle - \pi L[x, z] + \pi \langle J[x, z] | \chi[x, z]^{-1} | J[x, z] \rangle \right\} \times$$

$$\times 2 \cos \left\{ \frac{1}{\hbar} \langle p\lambda | \chi^{-1}[x] | J[x] \rangle \right\}. \quad (15)$$

Wigner function in this expression is determined by integral over all closed trajectories $z(\tau)$, which start and end in the origin x , as we have split trajectories on the “external” coordinate x

and “internal” coordinates $z(\tau)$ by the substitution $\bar{x}(\tau) = x/\lambda + z(\tau)$. Here scalar, vector and matrix functionals L , J and χ are

$$\begin{aligned} L[x, z] &= \int_0^1 d\tau \left[\dot{z}^2(\tau) + \frac{\beta}{\pi} U(x + \lambda z(\tau)) \right], \\ J[x, z] &= \frac{\beta\lambda}{2\pi} \int_0^1 d\tau \left(\tau - \frac{1}{2} \right) \frac{\partial U(y)}{\partial y} \Big|_{y=x+\lambda z(\tau)}, \\ \chi[x, z] &= \left[\hat{1} + \frac{\beta\lambda^2}{2\pi} \int_0^1 d\tau \left(\tau - \frac{1}{2} \right)^2 \frac{\partial^2 U(y)}{\partial y^2} \right] \Big|_{y=x+\lambda z(\tau)}. \end{aligned} \quad (16)$$

Note that the first term in exponent (15) looks explicitly like Maxwell distribution in classical statistics. The difference is in the matrix $\chi[x, z]$, which is reduced to unit matrix for free particle. Matrix $\chi[x, z]$ is also reduced to unit matrix in linear approximation accounting for only the first two terms in expansion (14).

2.4. Interpretation and applicability of harmonic approximation

The expression for Wigner function (15) is obtained under assumption, that potential $V(x + \lambda z(\tau) + \lambda \bar{\xi}(\tau - 1/2))$ is expanded in Taylor series up to the second order $\bar{\xi}$ with good accuracy. In the same time we neglected terms with higher power of $\bar{\xi}$. Thereby it is necessary to discuss the legality of such assumption. Primarily, note that variable $\bar{\xi}$ is in three positions in the exponent (13). The first one is Fourier term $i\langle p|\bar{\xi}\rangle/\hbar$, which makes momentum correlated with other dynamical variables. The second one is gaussian term $\pi\langle \bar{\xi}|\bar{\xi}\rangle$. The third one is integral term, where $\bar{\xi}$ is argument of potential $\int_0^1 d\tau \beta V(x + \lambda z(\tau) + \lambda \bar{\xi}(\tau - 1/2))$. Gaussian term provides rapid decay with increasing $\bar{\xi}$, so the main contribution comes from the region less or of order $\pi^{-1/2} \approx 0.6$. Moreover the argument of potential function contains $\bar{\xi}$ multiplied on factor $\tau - 1/2$, which is modulo less than 0.5. So using the mean value theorem, we can roughly estimate the high order terms of Taylor expansion in exponent (13) as

$$\frac{1}{n!} \frac{\partial^n V(x_0)}{\partial x^n} \int_0^1 d\tau \left(\tau - \frac{1}{2} \right)^n = \frac{1}{n!} \frac{(1 + (-1)^n)}{(n+1)2^{n+1}} \frac{\partial^n V(x_0)}{\partial x^n}, \quad (17)$$

where x_0 is certain point of trajectory. Numerical value of this integral rapidly decreases: when $n = 2, 4, 6$ it equals $1/24$, $1/1920$ and $1/322560$. Thus we expect negligible contribution of high order Taylor terms in potential expansion. Numerical test calculations for a lot of potentials confirm this hypothesis [26].

Note that the first summand in exponent (15) is similar to Maxwell distribution in classical statistics. The difference is in coefficient $\chi^{-1}[x, z]$.

2.5. Average values of quantum operators

Average value of arbitrary quantum operator \hat{A} can be written as Weyl's symbol $A(p, x)$, averaged over phase space with the Wigner function $W(p, x; \beta)$ as weight:

$$\langle \hat{A} \rangle = \int \frac{dp dx}{2\pi\hbar} A(p, x) W(p, x; \beta), \quad (18)$$

where the Weyl's symbol of operator \hat{A} is:

$$A(p, x) = \int \frac{ds}{2\pi\hbar} e^{i(s|x|)/\hbar} \langle p + s/2 | \hat{A} | p - s/2 \rangle. \quad (19)$$

Weyl's symbols for usual operators like \hat{p} , \hat{x} , \hat{p}^2 , \hat{x}^2 , \hat{H} , \hat{H}^2 etc. can be easily calculated directly from definition (19). For calculation of $\langle \hat{A} \rangle$ we are going to use the harmonic approximation of the Wigner function in path integral representation (15).

For making use of the Monte Carlo method (MC) [27, 28] we have to represent path integrals in discrete form of multiple integral. As a result we obtain final expressions for MC calculations in the following form:

$$\langle \hat{A} \rangle = \frac{\langle A(p, x) \cdot h(p, x, z_1, \dots, z_{M-1}) \rangle_w}{\langle h(p, x, z_1, \dots, z_{M-1}) \rangle_w}. \quad (20)$$

Here brackets $\langle g(p, x, z_1, \dots, z_{M-1}) \rangle_w$ denote averaging of any function $g(p, x, z_1, \dots, z_{M-1})$ with positive weight $w(p, x, z_1, \dots, z_{M-1})$:

$$\langle g(p, x, z_1, \dots, z_{M-1}) \rangle = \int dp dx \int dz_1 \dots dz_{M-1} g(p, x, z_1, \dots, z_{M-1}) w(p, x, z_1, \dots, z_{M-1}). \quad (21)$$

while

$$\begin{aligned} w(p, x, z_1, \dots, z_{M-1}) &= \left| \cos \left\{ \frac{\langle p \lambda | \chi_M^{-1}[x, z] | J_M[x, z] \rangle}{\hbar} \right\} \right| \times \\ &\times \exp \left\{ -\beta \frac{\langle p | \chi_M^{-1}[x, z] | p \rangle}{2m} - \pi L_M[x, z] + \pi \langle J_M[x, z] | \chi_M^{-1}[x, z] | J_M[x, z] \rangle \right\}, \\ h(p, x, z_1, \dots, z_{M-1}) &= \text{sign} \left(\cos \left\{ \frac{\langle p \lambda | \chi_M^{-1}[x, z] | J_M[x, z] \rangle}{\hbar} \right\} \right) \sqrt{\chi_M[x, z]}. \end{aligned}$$

Note that denominator in (20) is equal to nominator with $A(p, x) = 1$, so $C(M)$ from (12) is canceled.

3. Results of numerical calculations

To obtain preliminary results and to test the developed approach we have carried out calculations of the path integral representation of Wigner function in the framework of the mentioned above linear approximation. Calculations have been done for two hundred particles each presented by twenty beads. Results have been obtained by averaging-out over one million particle configurations.

Calculations have been done for ideal and strongly coupled electron-hole plasmas with effective hole mass equal to $100m_e$ at temperature $T = 0.3Ha$ and density related to the Wigner-Seitz radius equal to two ($r_s = 2$). Related coupling parameter is equal to 1.66.

We define the momentum distribution function for holes ($a = h$) and electrons ($a = e$) by the following expression:

$$g(|p_a|) = \frac{1}{N} \int_V dp dx \delta(p_{1,a} - p) W(p, x; \beta), \quad (22)$$

with normalization factor N equal to: $N = Z(\beta) = \int_V dp dx W(p, x; \beta)$.

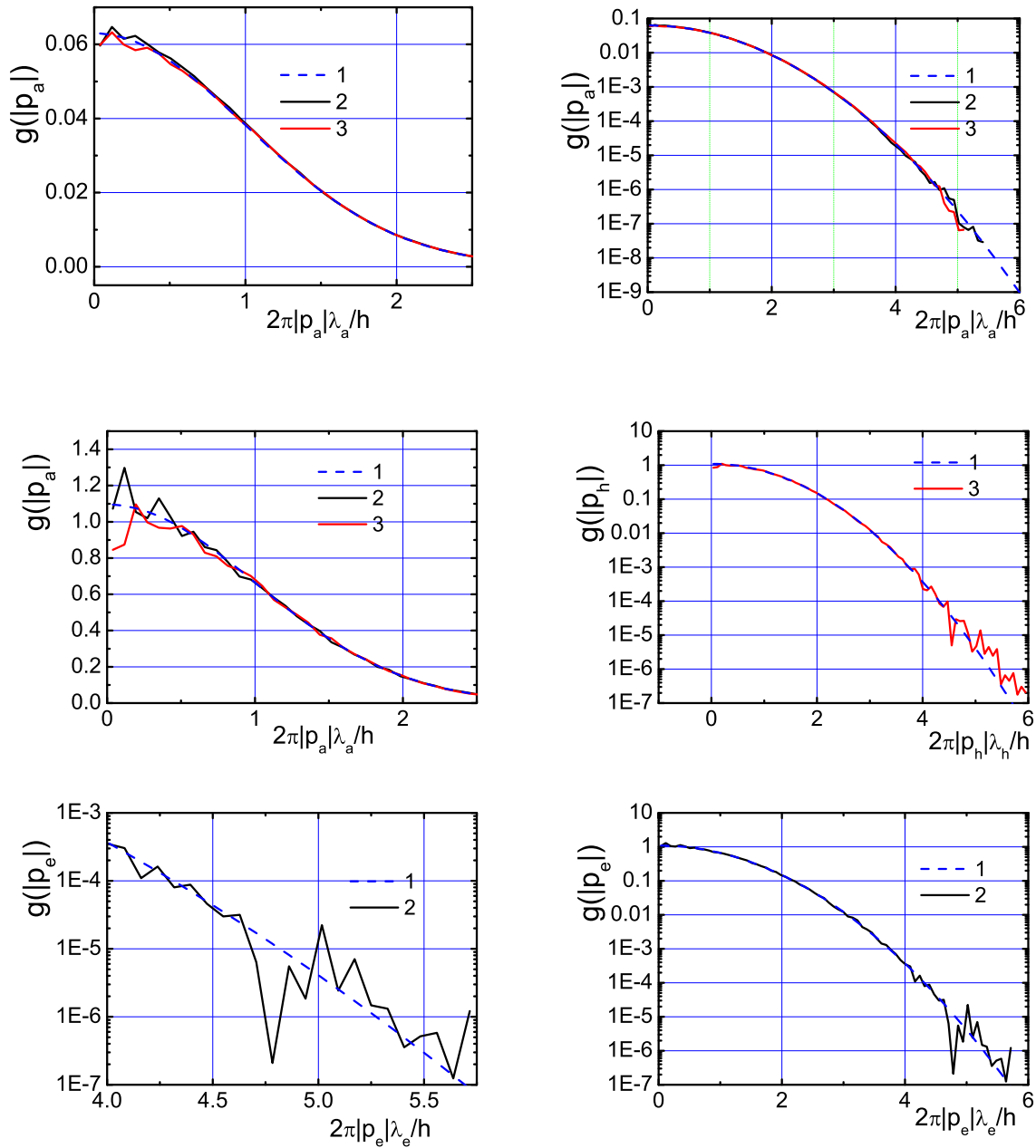


Figure 2. The electron ($a = e$) and hole ($a = h$) momentum distribution Wigner functions. The blue dashed line (1) show distribution function of ideal plasma. The black (2) and red (3) solid lines present the electron $g(|p_e|)$ and hole $g(|p_h|)$ distribution functions.

Let us note that the Wigner function is real valued function. For ideal and non-ideal electron–hole plasmas figure 2 shows electron and hole distribution functions $g_a(|p_a|)$, ($a = e, h$) versus the momentum scaled by the related thermal wavelength. Comparison of the ideal Maxwell–Boltzmann distribution function with results of our calculations for ideal plasma (see left and right upper panels of figure 2) demonstrate very good accuracy of our approach in wide range of particle momentum, in which decay of the distribution functions is about of six orders of magnitude (see two upper panels in figure 2).

The middle and bottom panels show the influence of the strong interparticle interaction on momentum distribution functions resulted in appearance of sharp oscillations. In the large momentum tails of electron distributions these sharp oscillations of one order of magnitude arise due to the interference of quantum effects, which are accounted for by the “cosine factor” in equation (15). For small momentums the “cosine factor” is close to unity and MC distribution functions approach practically the Maxwell–Boltzmann distribution.

On the whole presented normalized to unity distribution functions $g_a(|p_a|)$ resemble the related Maxwell–Boltzmann function. However to conserve normalization factor the sharp peaks of the MC distribution functions have to be compensated by the pits below Maxwell–Boltzmann function.

The physical reasons of the around ten percent oscillations of the distribution functions in vicinity of zero momentum have to be investigated in later publications.

4. Conclusion

In our work we have derived the new path integral representation of Wigner function of the Coulomb system of particles for canonical ensemble. We have obtained explicit expression of Wigner function in linear and harmonic approximation resembling the Maxwell–Boltzmann distribution on momentum variables, but with quantum corrections depending on the second derivatives of interparticle potential. This approximation contains also the oscillatory multiplier describing quantum interference. We have developed new quantum Monte-Carlo method for calculations of average values of arbitrary quantum operators. Preliminary calculations of the momentum distribution function for non-ideal plasma has been done. Comparison with classical Maxwell–Boltzmann distribution shows the significant influence of the quantum effects on the high energy asymptotics (“tails”) of the calculated momentum distribution functions resulted in appearance of sharp large scale oscillations.

Acknowledgments

We acknowledge stimulating discussions with professor M Bonitz and professor V I Man’ko. This work has been supported by the Russian Science Foundation (grant 14-50-00124).

References

- [1] Stefanucci G and Van Leeuwen R 2013 *Nonequilibrium Many-Body Theory of Quantum Systems. A Modern Introduction* (Cambridge: University Press)
- [2] Fortov V E 2011 *Extreme States of Matter: On Earth and in the Cosmos* (Berlin: Springer-Verlag)
- [3] Galitskii V M and Yakimets V V 1967 *Zh. Eksp. Teor. Fiz.* **51** 957
- [4] Eletskii A V *et al* 2005 *Phys. Usp.* **48** 281
- [5] Wigner E P 1932 *Phys. Rev.* **40** 749
- [6] Tatarskii V 1983 *Sov. Phys. Usp.* **26** 311
- [7] Shifren L and Ferry D K 2001 *Phys. Lett. A* **285** 217
- [8] Shifren L and Ferry D K 2002 *J. Comput. Electron.* **1** 55
- [9] Shifren L and Ferry D K *Physica B* **314** 72
- [10] Querlioz D and Dollfus P 2010 *The Wigner Monte-Carlo Method for Nanoelectronic Devices: A Particle Description of Quantum Transport and Decoherence* (John Wiley & Sons)
- [11] Sellier J M *et al* 2014 *Monte Carlo Meth. Appl.* **20** 43
- [12] Sellier J M and Dimov I 2015 *J. Comput. Phys.* **280** 287
- [13] Filinov V S *et al* 2012 *Phys. Lett. A* **376** 1096
- [14] Filinov V S *et al* 2013 *Phys. Rev. C* **87** 035207
- [15] Filinov V S *et al* 2015 *Plasma Phys. Control. Fusion* **57** 0440041
- [16] Zamalin V M and Norman G E 1973 *USSR Comp. Math. Math. Phys.* **13** 169
- [17] Wiener N 1923 *J. Math. Phys. (Cambridge, Mass.)* **2** 131
- [18] Feynman R P and Hibbs A R 1965 *Quantum mechanics and path integrals* (New York: McGraw-Hill)
- [19] Filinov V S *et al* 2007 *Phys. Rev. E* **75** 036401
- [20] Filinov V S *et al* 2001 *Plasma Phys. Contr. Fusion* **43** 743

- [21] Kelbg G 1963 *Ann. Physik* **12** 219
- [22] Ebeling W *et al* 1967 *Contrib. Plasma Phys.* **7** 233
- [23] Filinov A V *et al* 2004 *Phys. Rev. E* **70** 046411
- [24] Ebeling W *et al* 2006 *J. Phys. A: Math. Gen.* **39** 4309
- [25] Klakow D *et al* 1994 *Phys. Lett. A* **192** 55
- [26] Larkin A S, Filinov V S and Fortov V E 2016 *Contrib. Plasma Phys.* **56** 187–196
- [27] Metropolis N *et al* 1953 *J. Chem. Phys.* **21** 1087
- [28] Hasting W K 1970 *Biometrika* **57** 97